Applied Radiation and Isotopes 122 (2017) 116–120

Contents lists available at ScienceDirect

Applied Radiation and Isotopes

journal homepage: www.elsevier.com/locate/apradiso

Gamma-gamma coincidence performance of $LaBr_3$:Ce scintillation detectors vs HPGe detectors in high count-rate scenarios

A. Drescher[a], M. Yoho[a], S. Landsberger[a,*], M. Durbin[a], S. Biegalski[a], D. Meier[b], J. Schwantes[b]

[a] The University of Texas at Austin, Nuclear Engineering Teaching Laboratory, Pickle Research Campus R-9000, Austin, TX 78712, USA
[b] Pacific Northwest National Laboratory, 01 Battelle Blvd, Richland, WA 99352, USA

A R T I C L E I N F O

Keywords:
Gamma-gamma coincidence
$LaBr_3$:Ce scintillation
Gamma spectroscopy
High count rate
HPGe

A B S T R A C T

A radiation detection system consisting of two cerium doped lanthanum bromide ($LaBr_3$:Ce) scintillation detectors in a gamma-gamma coincidence configuration has been used to demonstrate the advantages that coincident detection provides relative to a single detector, and the advantages that $LaBr_3$:Ce detectors provide relative to high purity germanium (HPGe) detectors. Signal to noise ratios of select photopeak pairs for these detectors have been compared to high-purity germanium (HPGe) detectors in both single and coincident detector configurations in order to quantify the performance of each detector configuration. The efficiency and energy resolution of $LaBr_3$:Ce detectors have been determined and compared to HPGe detectors. Coincident gamma-ray pairs from the radionuclides ^{152}Eu and ^{133}Ba have been identified in a sample that is dominated by ^{137}Cs. Gamma-gamma coincidence successfully reduced the Compton continuum from the large ^{137}Cs peak, revealed several coincident gamma energies characteristic of these nuclides, and improved the signal-to-noise ratio relative to single detector measurements. $LaBr_3$:Ce detectors performed at count rates multiple times higher than can be achieved with HPGe detectors. The standard background spectrum consisting of peaks associated with transitions within the $LaBr_3$:Ce crystal has also been significantly reduced. It is shown that $LaBr_3$:Ce detectors have the unique capability to perform gamma-gamma coincidence measurements in very high count rate scenarios, which can potentially benefit nuclear safeguards in situ measurements of spent nuclear fuel.

1. Introduction

Characterization of spent and reprocessed nuclear fuel presents several challenges to conventional HPGe single detector gamma spectroscopy. Three challenges directly addressed using coincident $LaBr_3$:Ce scintillators are: 1) high count rates that result in significant dead time limiting the rate of data collection and reducing statistical precision; 2) gamma spectra containing a large, diverse, range of fission products complicates peak identification due to interference and intense Compton scattering; 3) transportation of spent nuclear fuel is expensive and time-intensive due to regulatory and safety concerns. These challenges place emphasis on the need for a system with strong background suppression, the best achievable energy resolution, and portability. Simulated gamma-ray spectrum deconvolution performed using a 2.54 cm x 2.54 cm (1 in. x 1 in.) cerium doped lanthanum-bromide ($LaBr_3$:Ce) detector was used to nondestructively determine the burn-up of spent nuclear fuel from the Advanced Test Reactor (ATR) on-site (Navarro et al., 2014).

Cerium doped lanthanum bromide ($LaBr_3$:Ce) is an excellent detector choice to potentially meet all of the above mentioned criteria. The efficiency of $LaBr_3$:Ce detectors is superior to that of thallium doped sodium-iodide detectors (NaI:*Tl*) (Saint Gobain, 2009). $LaBr_3$:Ce detectors have been shown to be 1.2–1.65 times more efficient than NaI:*Tl* detectors above 350 keV, for 3.8 cm × 3.8 cm (1.5 in. × 1.5 in.) detectors (Ciupek et al., 2014). The energy resolution of $LaBr_3$:Ce detectors is superior to that of NaI:*Tl* detectors (Saint Gobain, 2009). $LaBr_3$:Ce detectors have an energy resolution of 2.5–3% at the 662 keV gamma-line of ^{137}Cs, compared to 6–7% for NaI:*Tl* detectors (Ciupek et al., 2014). These advantages over NaI:*Tl* detectors have been demonstrated in an experiment which shows that $LaBr_3$:Ce detectors find more distinguishable peaks than NaI:*Tl* detectors with a higher efficiency (Milbrath et al., 2006). The lack of need for nitrogen cooling also makes $LaBr_3$:Ce systems significantly more portable than HPGe. $LaBr_3$:Ce has been shown to be an excellent detector choice for high count rate scenarios, and is capable of performing well with count rates up to 500 kHz (Löher et al., 2012). In the past, MCNPX calculations have been utilized to verify that $LaBr_3$:Ce scintillators can accurately identify isotopes in a fuel element spectrum (Navarro et al., 2014).

* Corresponding author.
E-mail address: s.landsberger@mail.utexas.edu (S. Landsberger).

http://dx.doi.org/10.1016/j.apradiso.2017.01.012
Received 20 July 2016; Received in revised form 3 January 2017; Accepted 15 January 2017
Available online 15 January 2017
0969-8043/

These results suggest that $LaBr_3$:Ce detectors will be useful in the characterization of spent nuclear fuel as well.

There are challenges associated with using $LaBr_3$:Ce detectors. First, $LaBr_3$:Ce is itself radioactive, due to natural abundances of lanthanum containing radioactive ^{138}La (Saint Gobain, 2009) (Ciupek et al., 2014). ^{138}La accounts for 0.09% of naturally occurring lanthanum and produces two gamma rays: a 788.7 keV gamma-ray from beta decay to ^{138}Ce, and a 1435.8 keV gamma ray from electron capture to ^{138}Ba. ^{138}La has a 1.06×10^{11} year half-life, and thus has activity concentrations of 0.065 Bq/cm^3 and 0.068 Bq/cm^3 for its two photopeaks respectively.

These intrinsic photopeaks degrade the detection limits at and below these energies during typical single-channel spectrum collection (Saint Gobain, 2009). In principle, these background features could be subtracted from single-channel spectra. However, this would create additional statistical uncertainties in the remaining results. Therefore, the preferred method of background elimination is gamma-gamma coincidence gating. One advantage to this internal radioactivity is that it provides a means of self-calibration of energies up to nearly 3000 keV. This advantage is particularly useful for autonomous portable systems that may not always have access to standard gamma sources in a typical laboratory setting, and is unique to $LaBr_3$:Ce scintillators (Xiang, 2013). It will also be shown that gamma-gamma coincidence methods are effective for eliminating the contributions from inherent radioactivity when self-calibration is not required.

A coincidence configuration of these detectors will be used for deconvolution of peaks and reduction of background, allowing for more precise characterization of complex spectra. Gamma-gamma coincidence has the advantage of virtually eliminating all background peaks that do not exist in coincidence with other peaks, significantly improving detection limits of useful radionuclides (Yoho and Landsberger, 2016, Horne and Landsberger, 2011). The disadvantage of this method is that it can only be applied to the detection of isotopes with coincident decay schemes. By employing gamma-gamma coincidence, the background from the radioisotopes in the $LaBr_3$:Ce scintillator is eliminated, providing a means for improving detection limits.

Resulting from a lack of readily available spent nuclear fuel, experiments were performed on a superposition of radioactive sources representing a high count rate and complicated spectrum, thus artificially simulating the potential situation of spent nuclear fuel. Experiments were performed with a single $LaBr_3$:Ce detector, a single HPGe detector, coincident $LaBr_3$:Ce detectors, and coincident HPGe detectors. Count rates were varied from 20 to 400 kHz. Sources included 50 mCi of ^{137}Cs, and 10 μCi of ^{133}Ba and ^{152}Eu. This combination of configurations provides multi-variate comparators to benchmark the signal-to-noise performance of each detector type as a function of: number of detectors, input count rate, and energy.

2. Experimental setup

2.1. Apparatus

The Nuclear Engineering Teaching Lab (NETL) at The University of Texas at Austin (UT Austin) has obtained two identical Saint Gobain Brillance 380 $LaBr_3$:Ce scintillation detectors with 38 mm x 38 mm cylindrical crystals and AS20 voltage dividers with analog signal output for use in a coincidence configuration. NETL is also equipped with two HPGe detectors in a coincidence configuration. Coincidence data processing was achieved with an XIA LLC Digital Gamma Finder Pixie-4 card. The DGF Pixie-4 is a multichannel data acquisition system for coincident radiation detection which assigns timestamps with a 13.3 ns timing resolution to each detected event (XIA LLC, 2013). Fig. 1 is a block diagram of the experimental setup for the coincidence $LaBr_3$:Ce detectors. The block diagram for HPGe detectors has no practical difference and is excluded.

The data collection interface is the Igor Pro program that operates

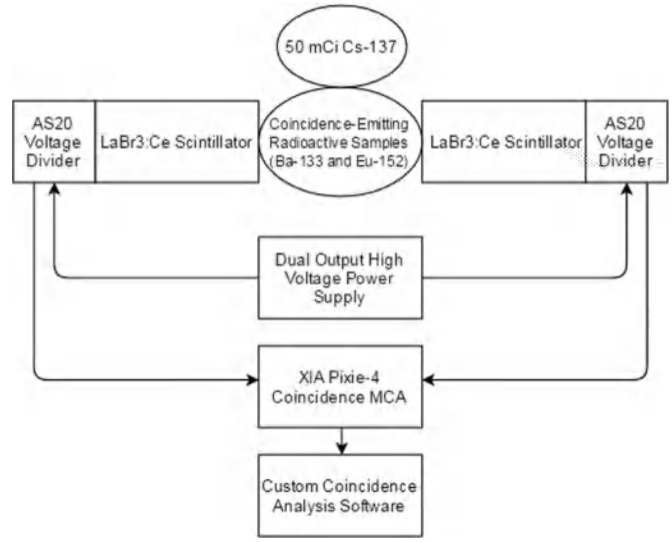

Fig. 1. $LaBr_3$:Ce Block Diagram.

the XIA Pixie-4 system. The software includes an adjustable coincidence timing window, which specifies the maximum time between two events that are registered as coincident. A procedure for optimizing the coincidence timing window for each detector type was developed, and will be presented. The manufacturer of the $LaBr_3$:Ce detectors list the efficiency as 143% vs NaI:*Tl*, and optimum energy resolution as 2.1% at 1332.5 keV ^{60}Co photopeak. (Saint Gobain, 2009).

2.2. Data collection and analysis

Data were collected in order to compare the following properties of $LaBr_3$:Ce and HPGe detectors: timing performance, efficiency, energy resolution, background elimination via coincidence gating, single detector peak signal to noise ratio (SNR), and coincidence configuration peak SNR.

2.2.1. Timing performance

Timing performance of the two detector types was compared by counting a ^{60}Co source while varying the adjustable coincidence timing window setting in the Igor Pro software. According to the decay scheme of ^{60}Co, the 1173.3 keV gamma-ray in coincidence with 1332.5 keV gamma-ray represents a true coincidence event, while 1173.3 keV gamma-ray in coincidence with itself, or 1332.5 keV gamma-ray in coincidence with itself represents a false coincidence event. Therefore, comparing the magnitude of peaks at true and false coincidence energy coordinates as seen in Fig. 2 provides an SNR, which is a useful metric to quantify the coincidence timing performance of each detector type for a range of timing window settings, and thus determine the optimum timing window setting for each detector type. Fig. 2.

Fig. 3 shows the results from measuring this SNR at varying timing windows. The optimum coincidence windows for HPGe and $LaBr_3$:Ce detectors are 26.6 and 13.3 ns, respectively. It should be noted that the XIA Pixie-4 is only capable of producing timing windows with a resolution of 13.3 ns. It is therefore likely that the optimum $LaBr_3$:Ce timing window was not achieved, and exceeds the capabilities of current instrumentation. There exists an XIA Digital Gamma Finder Pixie-500 with a clock of 500 MHz. If acquired, it is expected that this would significantly improve the performance of the $LaBr_3$:Ce detectors. The performance of HPGe detectors on the other hand was optimized at about 26 ns, and dropped considerably when reducing the timing window from 26.6 to 13.3 ns. These timing windows will be used for all coincident SNR comparisons between the two detector types that follow.

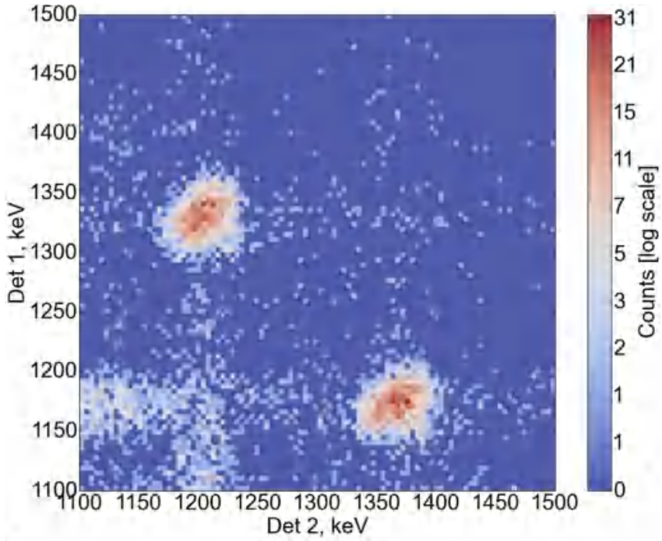

Fig. 2. ^{60}Co coincidence heatmap. The energy coordinates at (1173, 1173) and (1332, 1332) represent false coincidence events, while (1173, 1332) and (1332, 1172) represent true coincidence events.

2.2.2. Efficiency and energy resolution

A collection of certified monoenergetic gamma sources was utilized in the determination of detector efficiency and energy resolution. These sources were provided by Eckert & Zeigler, and include ^{241}Am, ^{109}Cd, ^{139}Ce, ^{203}Hg, ^{113}Sn, ^{137}Cs, ^{54}Mn, ^{65}Zn, and ^{60}Co. Each source was counted on each detector at a distance of 10 cm for 300 s. This distance was chosen in order to minimize dead-time and pile-up while still maintaining Gaussian peaks with a net area of at least 3000 counts. The geometry of the counting setup was preserved between the two detector types. The activities of all sources were below 1 µCi, therefore dead-time and true coincidence summing effects were negligible. The HPGe detector utilized was a GMX35P4–70 n-type cylindrical detector with dimensions of 55.9 mm × 57.5 mm. A comparison of the efficiency and resolution of the $LaBr_3$:Ce and HPGe detectors, are shown in Fig. 4 and Fig. 5, respectively.

The HPGe detector has superior energy resolution and efficiency to the $LaBr_3$:Ce detector. Energy resolution values were obtained by using ORTEC Maestro's built-in peak identification functionality in order to identify the peak locations and full-width half maximum (FWHM) values.

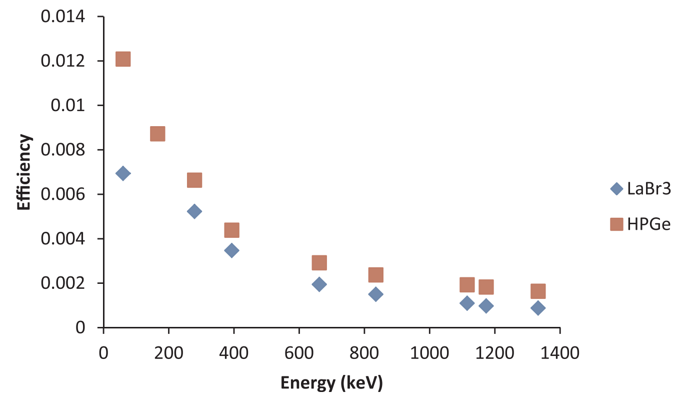

Fig. 4. A comparison of the efficiency of $LaBr_3$:Ce and HPGe detectors.

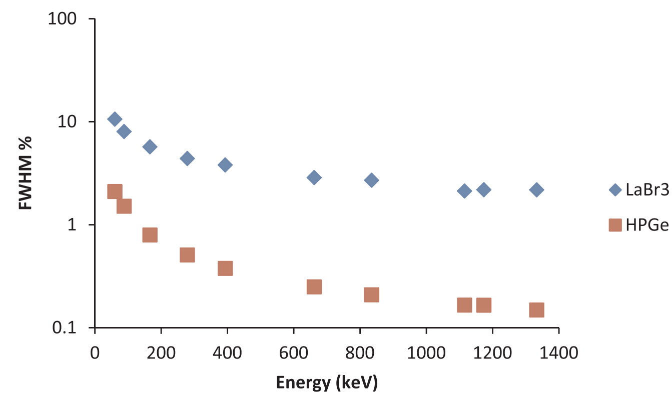

Fig. 5. A comparison of the energy resolution of LaBr3:Ce and HPGe detectors.

2.2.3. Background elimination via coincidence gating

The peaks in this background spectrum (Fig. 6) include 1435.8 keV photon, which is the result of ^{138}La decaying after electron capture to ^{138}Ba (66.4%), a 788.7 keV photon, which is the result of ^{138}La

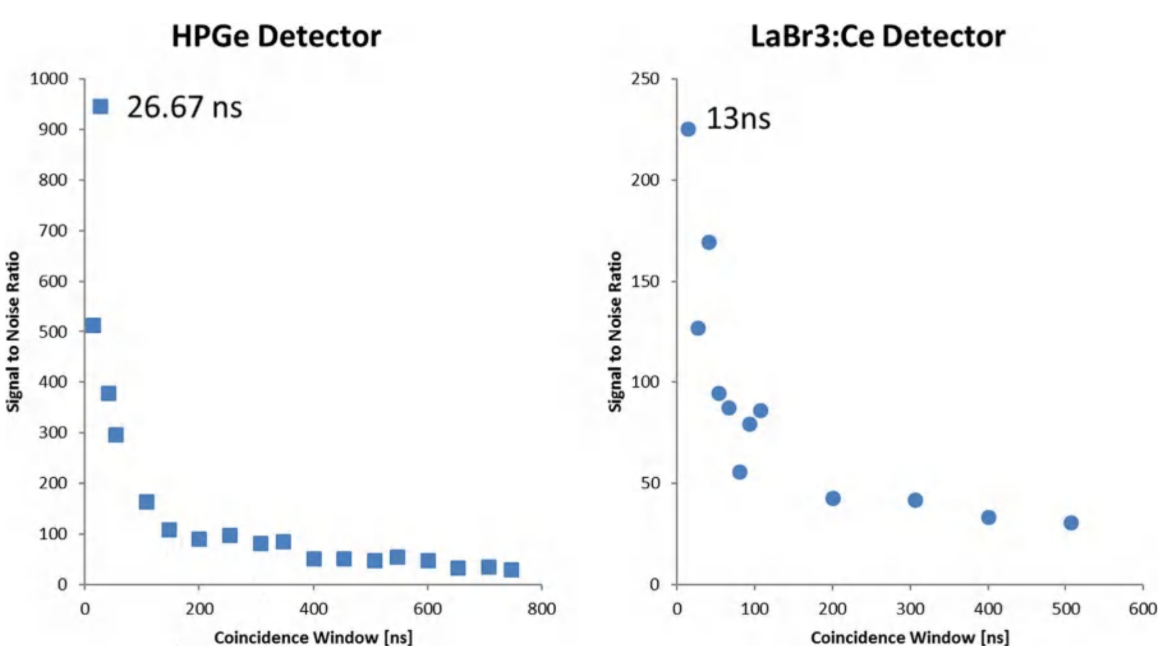

Fig. 3. SNR vs coincidence timing window for the HPGe and $LaBr_3$:Ce detectors.

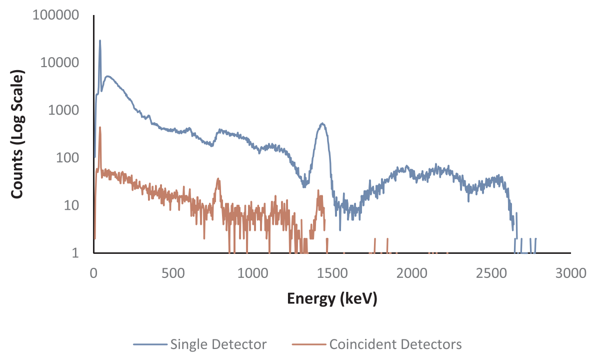

Fig. 6. Background spectrum characteristic of LaBr3:Ce detectors. The top curve represents a background spectrum collected with a single $LaBr_3$:Ce detector. The bottom curve represents a background spectrum collected with coincident $LaBr_3$:Ce detectors, with a coincidence gate applied over the energy range 5–2900 keV. (It should be noted that both curves represent the same dataset. The coincidence curve just applies additional gating logic.).

decaying by beta-emission to ^{138}Ce (33.6%), and a 34.8 keV ^{138}Ba x-ray, which is the result of the averaged captured electron's shell being refilled (kα2, kα2., kβ3, kβ1, and kβ2). Aside from the associated Compton continuums and other consequences of these peaks, the rest of the peaks of this spectrum are standard background ones that would be present in the spectrum of any unshielded detector. A basic application of gamma-gamma coincidence involves gating over the entire range of this spectrum. By creating a gate 3000 keV wide, gamma rays only appear in the spectrum if they are coincident with any other gamma ray as shown in the lower curve in Fig. 6.

Upon applying this energy gate, the 1435.8 keV peak has been reduced by an order of magnitude. Counts across the entire spectrum have similarly been reduced by an order of magnitude or more. Therefore, coincidence gating results in a significant reduction in background. This is particularly advantageous for $LaBr_3$:Ce detectors due to their strong intrinsic radioactivity. Similar energy gating methods can be utilized to de-convolve high activity spectra, as will be shown next.

2.2.4. Single and dual detector peak SNR

Having established a proof-of-concept of coincidence methodologies for simplifying a background spectrum, the next stage in this experiment is to artificially create a complicated high activity spectrum to quantify the performance of each detector configuration. SNR's of select gamma-ray peaks were measured with single and dual $LaBr_3$:Ce and HPGe detectors for a range of count rates. The 1850 MBq (50 mCi) ^{137}Cs source contains a shutter that can be adjusted to attenuate the gamma radiation to different levels. Changing this shutter position allowed count rates of the experimental setup to vary from 20 to 400 kHz.

Three sample activity levels were measured (by varying the ^{137}Cs shutter position) with both detector types in single and dual detector configurations. The activity levels will be denoted “Low Count Rate” (LCR), “High Count Rate” (HCR), and “Very High Count Rate” (VHCR). Each data collection was performed for one hour. The following photopeak pairs from ^{152}Eu and ^{133}Ba were selected, and their SNR was measured for each count rate, detector type, and detector configuration. The gamma-ray pairs are shown in Table 1.

3. Results

SNR's for the coincident photopeak energy pairs tabulated above were calculated for all of the single and dual detector measurements taken. SNR's were calculated by selecting each photopeak as a region of interest in the ORTEC Maestro software. The signal was defined as the gross area of each photopeak, and the noise was defined as the difference between gross and net areas. SNR was then calculated as the ratio of the

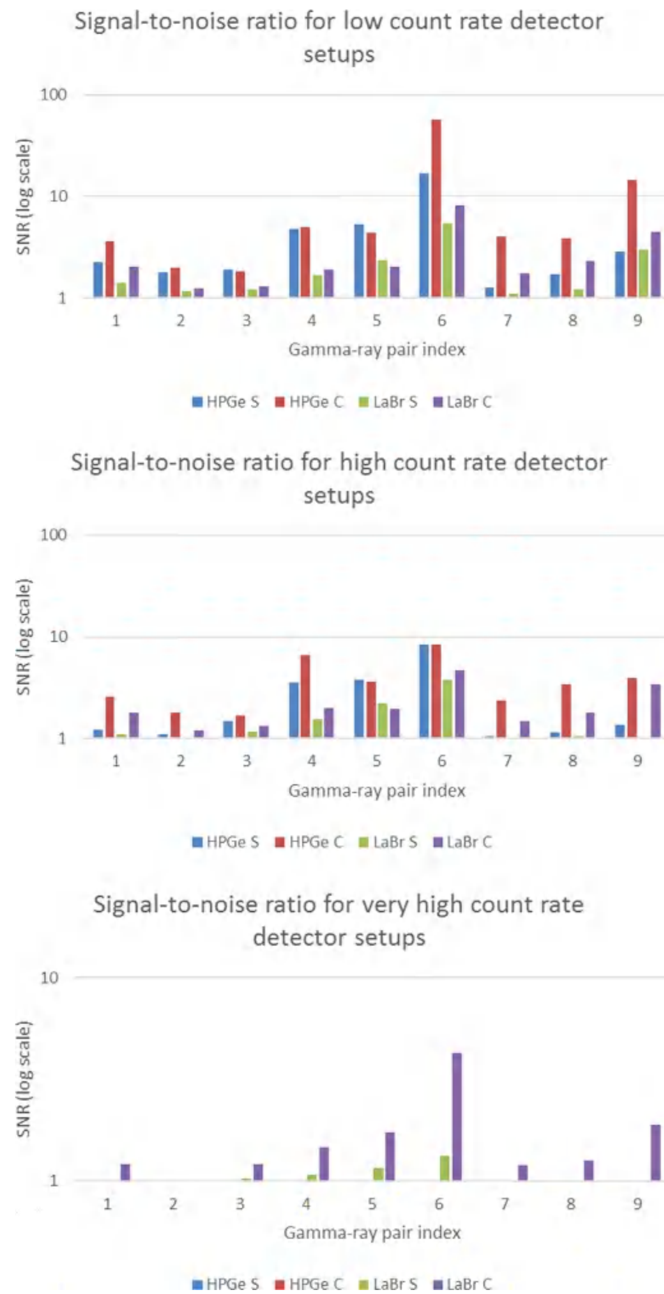

Fig. 7. Signal-to-noise ratios for all detector setups for low, high, and very high count rates. The pair of coincident gamma-rays corresponding to each index are the pairs of gamma-rays listed in Table 1 in order.

defined signal and noise. The following charts in Fig. 7 show the results of the SNR calculations. Note that the SNR improvements vary greatly between gamma-ray pairs. This is a result of the differing decay schemes between each coincidence pair. The capability of coincident measurements to improve SNR is highly dependent on the fractional intensity of the coincidence gamma-ray pair. For gamma-ray pairs that have much lower coincident intensities relative to their independent intensities, the improvement from employing coincidence measurements is reduced. In particular, gamma-ray pairs 5 and 6 have very low coincidence intensities relative to their independent intensities.

The results also show that, in general, the improvements obtained by employing coincidence measurements are greater in magnitude for higher count rates scenarios. The HCR improvements in SNR for both detector types are generally greater than the LCR improvements in SNR. The most dramatic evidence for this is in the VHCR case. Only $LaBr_3$:Ce detectors in coincidence were capable of detecting almost all of the

Table 1
A list of the coincident photopeaks selected for measurement.

Nuclide	Coincident Photopeak Energy Pairs [keV]
^{152}Eu	(121, 244), (121, 444), (121, 867), (121, 965), (121, 1112), (121, 1408)
^{133}Ba	(80, 276), (80, 303), (80, 356)

gamma-rays. HPGe detectors at this activity level were fully paralyzed. Table 1.

4. Summary and conclusions

These data show that coincidence configurations result in substantial SNR improvements over single detector configurations for gamma-rays that characteristically decay in coincidence with high intensity relative to their independent decay intensities. These data demonstrate that, for complicated measurements of photopeaks subject to substantial interferences from other sources, if those photopeaks exist in coincidence it is of great benefit to exploit gamma-gamma coincidence counting.

At lower count rates, HPGe detectors have superior SNR to $LaBr_3$:Ce detectors. However, in very high count rate regimes, HPGe detectors are unable to perform. There are no data for VHCR HPGe detectors because this activity level fully paralyzed the detectors. The maximum count rate that was successfully measured with HPGe detectors was about 150 kHz. By comparison, $LaBr_3$:Ce detectors successfully measured data at over 400 kHz. This demonstrates that, for very high count rate scenarios, only $LaBr_3$:Ce detectors are sufficient. For safeguards analysis, such as in situ measurements of spent nuclear fuel, $LaBr_3$:Ce detectors are therefore an excellent option. Their portability, ability to handle extreme count rates, and excellent timing performance make them ideal for gamma-gamma coincidence measurements of very high activity samples such as spent nuclear fuel.

The ability to handle extreme count rates is of particular importance in coincidence counting. In single detector counting, moving the source further away from the detector reduces the count rate, and makes activity levels a non-issue. However, for coincidence counting, it is critical that the two detectors are as close to each other, and as close to the sample, as possible. This is because the efficiency of coincidence counting drops off as x^{-4}, where x is the source-detector distance. Count rate drops only as x^{-2}. There is therefore no benefit to moving coincidence detectors further away from the measured source. $LaBr_3$:Ce detectors therefore have the potential to fulfill the unique role of extending the capabilities of gamma-gamma coincidence spectroscopy to extreme count rate regimes on the order of 400 kHz or greater.

5. Future work

$LaBr_3$:Ce detectors will be used to measure fission products in irradiated uranium samples in order to back-calculate the uranium enrichment. This will be done for samples with count rates that preclude measurements on HPGe coincident detectors. This experiment will further demonstrate the capabilities of $LaBr_3$:Ce detectors to extract useful information in difficult measurement scenarios.

Acknowledgements

This work has been funded by Pacific Northwest National Lab. This material is based upon work supported by the Department of Energy National Nuclear Security Administration under Award Number DE-NA0002576.

References

Ciupek, K., Jednoróg, S., Fujak, M., Szewczak, K., 2014. Evaluation of efficiency for in situ gamma spectrometer based upon cerium-doped lanthanum bromide detector dedicated for environmental radiation monitoring. J. Radioanal. Nucl. Chem. 299, 1345–1350. http://dx.doi.org/10.1007/s10967-013-2906-z.

Horne, S., Landsberger, S., 2011. Selenium and mercury determination in biological samples using gamma–gamma coincidence and Compton suppression. J. Radioanal. Nucl. Chem. 291, 49–53. http://dx.doi.org/10.1007/s10967-011-1268-7.

Löher, B., Savran, D., Fiori, E., Miklavec, M., Pietralla, N., Vencelj, M., 2012. High count rate spectroscopy with LaBr3:Ce scintillation detectors. Nucl. Instrum. Methods Phys. Res. Sect. A Accel. Spectrometers, Detect. Assoc. Equip. 686, 1–6. http://dx.doi.org/10.1016/j.nima.2012.05.051.

Milbrath, B. D., Choate, B. J., Fast, J. E., Hensley, W. K., Kouzes, R. T., Schweppe, J. E., 2006. Comparison of LaBr3: Ce and NaI (Tl) scintillators for radio-isotope identification devices. http://citeseerx.ist.psu.edu/viewdoc/download?doi=10.1.1.558.8042&rep=rep1&type=pdf.

Navarro, J., Ring, T.A., Nigg, D.W., 2014. Gamma-ray simulated spectrum deconvolution of a LaBr3 1×1 in. scintillator for nondestructive ATR fuel burnup on-site predictions.〈http://www.osti.gov/pages/servlets/purl/1178058〉.

Saint Gobain Crystals, Scintillation Products Technical Note. 2009. http://www.crystals.saint-gobain.com/sites/imdf.crystals.com/files/documents/brillance_performance_summary.pdf.

XIA LLC, User's Manual Digital Gamma Finder (DGF) Pixie-4. 2013. http://www.xia.com/Manuals/Pixie4_UserManual.pdf.

Xiang, Q., Tian, D., Hao, F., Chu, C., Ding, G., Zeng, J., Luo, F., 2013. Self-calibration method for cerium-doped lanthanum bromide scintillator detector in the 0.1–2.0 MeV energy range. J. Radioanal. Nucl. Chem. 299, 1439–1445. http://dx.doi.org/10.1007/s10967-013-2782-6.

Yoho, M., Landsberger, S., 2016. Determination of selenium in coal fly ash via γ–γ coincidence neutron activation analysis. J. Radioanal. Nucl. Chem. 307, 733–737. http://dx.doi.org/10.1007/s10967-015-4209-z.